Signal Processing 89 (2009) 1990–1997

Contents lists available at ScienceDirect

Signal Processing

journal homepage: www.elsevier.com/locate/sigpro

Asymptotic optimal SINR performance bound for space–time beamformers ☆

Marc Oudin [a], Jean Pierre Delmas [b,*]

[a] Thales Airborne Systems, 2 Avenue Gay Lussac, 78990 Elancourt, France
[b] Institut TELECOM, TELECOM SudParis, Département CITI, UMR-CNRS 5157, 91011 Evry, France

ARTICLE INFO

Article history:
Received 27 December 2008
Received in revised form
27 March 2009
Accepted 1 April 2009
Available online 14 April 2009

Keywords:
Space–time beamforming
Asymptotic SINR
Performance analysis generalized eigenvalues
Block Toeplitz matrix
Szegö's theorem

ABSTRACT

In many detection applications, the main performance criterion is the signal to interference plus noise ratio (SINR). After linear filtering, the optimal SINR corresponds to the maximum value of a Rayleigh quotient, which can be interpreted as the largest generalized eigenvalue of two covariance matrices. Using an extension of Szegö's theorem for the generalized eigenvalues of Hermitian block Toeplitz matrices, an expression of the theoretical asymptotic optimal SINR w.r.t. the number of taps is derived for arbitrary arrays with a limited but arbitrary number of sensors and arbitrary spectra. This bound is interpreted as an optimal zero-bandwidth spatial SINR in some sense. Finally, the speed of convergence of the optimal wideband SINR for a limited number of taps is analyzed for several interference scenarios.

1. Introduction

Beamforming is used in many applications. It consists of spatially filtering signals, thanks to an array of sensors, and allows one to form "nulls" in the direction of interfering sources while maintaining a given gain in a desired direction. Usually, signals are narrowband [1] and spatial processing alone is sufficient (e.g., see [2]). However, in many applications, such as sonar, radar or communications, broadband signals are required to achieve desired performance, for instance in terms of range resolution or channel capacity. The counterpart is that it also leads to a loss in interference rejection performance (e.g., see [1,3]) and some sort of frequency compensation is required to keep good nulling performance. Therefore, space–time processing algorithms, which can be based on time or frequency-domain implementations, are used. Most of these algorithms are designed with the constraint that the signal is preserved through optimization criteria such as linearly constrained minimum variance (LCMV). However, since those algorithms are optimized under constraints, they are not optimal from the signal to interference plus noise ratio (SINR) point of view, which is the main performance criterion used for detection problems. Indeed, after linear filtering and under the current assumption that observation data are composed of signal of interest and additive Gaussian interference and noise, maximizing the SINR is equivalent to the Neyman–Pearson criterion. In this paper, we consider this context of detection problems. Thus, the objective of this paper is to study the performance of the optimal processing in the sense of SINR maximization.

When a linear filter is applied to observation data, the SINR corresponds to a Rayleigh quotient, associated with the covariance matrices of the signal of interest and interference plus noise components. Therefore, the optimal SINR corresponds to the maximum value of a Rayleigh quotient and can then be interpreted as the largest generalized eigenvalue of the two matrices. Thus, the problem of the optimal SINR computation is closely

☆ This work was supported in part by the French MOD (DGA) and in part by THALES/TR6/SR.

* Corresponding author. Tel.: +33 1 60 76 46 32; fax: +33 1 60 76 44 33.
E-mail addresses: marc.oudin@fr.thalesgroup.com (M. Oudin), jean-pierre.delmas@it-sudparis.eu (J. Pierre Delmas).

0165-1684/$ - see front matter © 2009 Elsevier B.V. All rights reserved.
doi:10.1016/j.sigpro.2009.04.004

related to the generalized eigenvalue problem. However, since the interpretation of the generalized eigenvalues of space–time covariance matrices with a finite number of taps is difficult, the analysis of the optimal SINR broadband beamforming does not easily lead to explicit expressions of the optimal SINR. This difficulty to analyze the performance of broadband beamformers with a finite number of taps has also been noted for optimal processing in the sense of other criteria such as minimum mean squared error (MMSE) or minimum variance distortionless response (MVDR). Many authors have studied the performance of time domain (e.g., see [5,6]) or frequency-domain implementations (e.g., see [12,7]) but, to the best of our knowledge, most analyses have been done through numerical simulations (e.g., see [5,6,8,9]) or for particular cases of arrays with temporally white signals (e.g., see [10]). However, we note that in some applications, the number of taps may be much larger than the number of sensors. For instance, in microphone array processing, where acoustic echoes of loudspeakers corrupt the desired signal, acoustic echo cancellers are often used, requiring a great number of taps (about 1000 taps or more), whereas the number of microphones is most of the time moderate (often less than 10 microphones, e.g., see [11]). Furthermore, if technology constraints impose the number of sensors, time filtering may be realized by different means, e.g., by recursive or subband filtering with different complexity/performance tradeoffs. In these conditions, an asymptotic approach in the number of taps seems justified. Moreover, contrary to the previous studies, this approach allows us to consider arrays of arbitrary geometry with a limited but arbitrary number of sensors and arbitrary interference and signal of interest spectra. Thus, we can compute a theoretical upper bound associated with an infinite number of taps, useful for comparisons with the SINR obtained after different space–time processing algorithms based for instance on FIR (e.g., see [4]), subband decomposition (e.g., see [12,13]), or IIR filters (e.g., see [14]).

In beamforming problems, if the observation data are modelled by second-order temporally stationary processes, space–time covariance matrices are block-Toeplitz structured. In this paper, we make use of that property to derive a closed-form expression of the asymptotic optimal SINR space–time beamformers. To proceed, we use an extension of the celebrated Szegö's theorem given by Grenander and Szegö [15] and revisited by Gray [16] which asserts that the eigenvalues of a sequence of Hermitian Toeplitz matrices asymptotically behave like the samples of the Fourier transform of its entries, to the generalized eigenvalues of a pair of Hermitian matrices that has been derived in [17,18]. This extended theorem allows one to characterize the generalized eigenvalue distribution of Toeplitz matrices and consequently many properties can be derived from it, such as for instance the asymptotic behavior of the minimum and maximum generalized eigenvalues. Using this theorem, we derive in this paper the expression of the asymptotic optimal space–time SINR w.r.t. the number of taps for a fixed number of sensors and give interpretations of the result in particular scenarios. Then, we complement theoretical results by numerical simulations that illustrate the convergence speed of the optimal SINR for a limited number of taps to its asymptotic optimal value in those scenarios.

This paper is organized as follows. In Section 2, the data model is presented and the expression and structure of the signal and interference plus noise covariance matrices is derived. Then, in Section 3, Szegö's theorem extended to the asymptotic behavior of the generalized eigenvalues of block Toeplitz matrices is recalled and applied to the performance analysis of optimal SINR space–time beamforming. Finally, in Section 4, illustrations by numerical examples are given to illustrate the convergence of the optimal SINR with a finite number of taps to the asymptotic one.

The following notations are used throughout the paper. Matrices and vectors are represented by bold upper case and bold lower case characters, respectively. Vectors are by default in column orientation, H stands for conjugate transpose. $\mathrm{Tr}(\cdot)$ and $\lambda_1(\cdot)\geqslant\cdots\geqslant\lambda_L(\cdot)$ denote the trace of a matrix and the decreasing ordered eigenvalues of an $L\times L$ matrix whose eigenvalues are real valued, respectively.

2. Data model

2.1. Data model

Let us consider an array composed of L sensors. We denote by B the bandwidth of the signals around the center frequency f_0. Then, we consider an environment composed of a signal of interest, a field of interference and thermal noise. These three signals are uncorrelated with each other. The interference and the thermal noise are modelled by non-zero-bandwidth second-order stationary processes and furthermore the thermal noise is spatially and temporally white, with power σ_n^2. The baseband, possibly correlated J interferers[1] have power spectral density (PSD) $(\mathscr{S}_j(f))_{j=1\ldots J}$ and cross power spectral density $(\mathscr{S}_{jj'}(f))_{j\neq j'=1\ldots J}$. The interference plus noise $L\times L$ spatial covariance matrix associated with the baseband received signal is equal to (e.g., see [4, Chapter 6])

$$\int_{-B/2}^{B/2}\left(\sum_{j=1}^{J}\mathscr{S}_j(f)\boldsymbol{\phi}(\theta_j,f)\boldsymbol{\phi}(\theta_j,f)^H + \sum_{1\leqslant j\neq j'\leqslant J}\mathscr{S}_{jj'}(f)\boldsymbol{\phi}(\theta_j,f)\boldsymbol{\phi}(\theta_{j'},f)^H\right)df+\sigma_n^2\mathbf{I}$$

with $\boldsymbol{\phi}(\theta_j,f)=[e^{jp\mathbf{r}_1^T\mathbf{i}(\theta_j)},e^{jp\mathbf{r}_2^T\mathbf{i}(\theta_j)},\ldots,e^{jp\mathbf{r}_L^T\mathbf{i}(\theta_j)}]^T$ where $(\mathbf{r}_\ell)_{\ell=1\ldots L}$ denotes a vector pointing from the origin to the ℓth sensor, $\mathbf{i}(\theta_j)$ a unit length arrival vector for an interference j in the direction θ_j and $p=2\pi(f_0+f)/c$ with c denoting the propagation speed of the wave. The signal of interest is also modelled by a non-zero-bandwidth second-order stationary process with PSD $\mathscr{S}_s(f)$. It is assumed to have a

[1] Note that this model includes arbitrary second-order stationary field of interference using specular approximations of diffuse interference, e.g., see [4, Section 5.5].

known direction of arrival (DOA) θ_s. Its $L \times L$ spatial covariance matrix may be written as

$$\int_{-B/2}^{B/2} \mathscr{S}_s(f)\boldsymbol{\phi}(\theta_s,f)\boldsymbol{\phi}(\theta_s,f)^H\,df \tag{1}$$

2.2. Expression of the space–time covariance matrices

Let K denote the number of taps used for temporal processing at each sensor at Shannon sampling rate $T = 1/B$. The interference plus noise and signal of interest space–time covariance matrices, respectively, $\bar{\mathbf{R}}_{i+n,K}$ and $\bar{\mathbf{R}}_{s,K}$ are of dimension $KL \times KL$. They are, respectively, Hermitian positive definite (due to the presence of thermal noise) and Hermitian positive semidefinite. Then, due to the second-order stationarity of the processes, these two space–time covariance matrices are block-Toeplitz structured and may be written as

$$\begin{bmatrix} \mathbf{R}_0 & \mathbf{R}_1^H & \cdots & \mathbf{R}_{K-1}^H \\ \mathbf{R}_1 & \ddots & \ddots & \mathbf{R}_{K-2}^H \\ \vdots & \ddots & & \vdots \\ \mathbf{R}_{K-1} & \mathbf{R}_{K-2} & \ldots & \mathbf{R}_0 \end{bmatrix} \tag{2}$$

where matrices $(\mathbf{R}_k)_{k=0,\ldots,K-1}$ are given for $\bar{\mathbf{R}}_{i+n,K}$ and $\bar{\mathbf{R}}_{s,K}$, respectively, by

$$\int_{-B/2}^{B/2}\left(\sum_{j=1}^{J}\mathscr{S}_j(f)\boldsymbol{\phi}(\theta_j,f)\boldsymbol{\phi}(\theta_j,f)^H + \sum_{1\leqslant j\neq j'\leqslant J}\mathscr{S}_{j,j'}(f)\boldsymbol{\phi}(\theta_j,f)\boldsymbol{\phi}(\theta_{j'},f)^H + \frac{\sigma_n^2}{B}\mathbf{I}\right)e^{-i2\pi kfT}\,df$$

and

$$\int_{-B/2}^{B/2}\mathscr{S}_s(f)\boldsymbol{\phi}(\theta_s,f)\boldsymbol{\phi}(\theta_s,f)^H e^{-i2\pi kfT}\,df$$

Let us note that the blocks $\mathbf{R}_k$ are not necessarily Toeplitz, depending on the structure of the array.

To apply the extended Szegö's theorem in the next section, we remark that the sequences $\mathbf{R}_k$ associated with the interference plus noise and the signal of interest are generated by the Fourier coefficients of the $L \times L$ Hermitian matrix valued functions

$$\mathbf{R}_{i+n}(f) = \sum_{j=1}^{J}\mathscr{S}_j(f)\boldsymbol{\phi}(\theta_j,f)\boldsymbol{\phi}(\theta_j,f)^H + \sum_{1\leqslant j\neq j'\leqslant J}\mathscr{S}_{j,j'}(f)\boldsymbol{\phi}(\theta_j,f)\boldsymbol{\phi}(\theta_{j'},f)^H + \frac{\sigma_n^2}{B}\mathbf{I} \tag{3}$$

and

$$\mathbf{R}_s(f) = \mathscr{S}_s(f)\boldsymbol{\phi}(\theta_s,f)\boldsymbol{\phi}(\theta_s,f)^H \tag{4}$$

respectively.

3. Expression of the asymptotic optimal space–time SINR

3.1. Expression of the space–time optimal SINR

Space–time beamforming consists in linearly filtering the LK-dimensional space–time data by a tap-stacked vector $\mathbf{w}_K$ when K taps are used. The optimal space–time processing (in the sense of SINR maximization) maximizes the generalized Rayleigh quotient:

$$\mathrm{SINR}(K) \overset{\mathrm{def}}{=} \max_{\mathbf{w}_K}\frac{\mathbf{w}_K^H\bar{\mathbf{R}}_{s,K}\mathbf{w}_K}{\mathbf{w}_K^H\bar{\mathbf{R}}_{i+n,K}\mathbf{w}_K} \tag{5}$$

where $\bar{\mathbf{R}}_{s,K}$ and $\bar{\mathbf{R}}_{i+n,K}$ are the space–time covariance matrices for the signal of interest and interference+noise signals, respectively, and given by (2). As noted in the previous section, $\bar{\mathbf{R}}_{s,K}$ and $\bar{\mathbf{R}}_{i+n,K}$ are, respectively, Hermitian positive semidefinite and Hermitian positive definite matrices. Therefore, the solution $\mathbf{w}_K$ of this optimization problem is given by the generalized eigenvector associated with the largest generalized eigenvalue of the couple $(\bar{\mathbf{R}}_{s,K}, \bar{\mathbf{R}}_{i+n,K})$. Then, the optimal space–time SINR is given by the largest generalized eigenvalue of $(\bar{\mathbf{R}}_{s,K}, \bar{\mathbf{R}}_{i+n,K})$ also corresponding to the largest eigenvalue λ_1 of $\bar{\mathbf{R}}_{i+n,K}^{-1}\bar{\mathbf{R}}_{s,K}$

$$\mathrm{SINR}(K) = \lambda_1(\bar{\mathbf{R}}_{i+n,K}^{-1}\bar{\mathbf{R}}_{s,K})$$

The value of this optimal SINR is difficult to interpret. Furthermore, closed-form expressions are not attainable, except in the trivial case of narrowband signals. Consequently, it will be insightful to consider the asymptotic (w.r.t. the number of taps) optimal SINR that will be used as an approximation for the upper bound of the SINR in the case of a finite number K of taps.

3.2. Expression of the asymptotic optimal SINR for arbitrary interference

To consider in the following the limit of the SINR w.r.t. K for arbitrary given interference and signal of interest DOAs, we use the following extension of Szegö's theorem (e.g., see [17, Theorem 3.9]; [18, Theorem 1]) that we recall for the convenience of the reader.[2]

Theorem 1. *Let $\mathbf{A}_{K,L}$ and $\mathbf{B}_{K,L}$ be two L block Toeplitz $KL \times KL$ Hermitian matrices with L fixed, such that $\mathbf{B}_{K,L}$ is positive definite, generated by absolutely summable sequences $\{a_n^{u,v}\}_{n=\ldots,-1,0,1,\ldots}$ and $\{b_n^{u,v}\}_{n=\ldots,-1,0,1,\ldots}$ with $u,v = 1,\ldots,L$ of Fourier transform $a^{u,v}(\omega) = \sum_n a_n^{u,v}e^{-in\omega}$ and $b^{u,v}(\omega) = \sum_n b_n^{u,v}e^{-in\omega}$, respectively. Let $\mathbf{A}(\omega)$ be the $L \times L$ matrix*

[2] We note that the highly sophisticated mathematical tools employed in [17] are sometimes beyond the grasp of the engineering community. Consequently the results obtained in this paper have not received appreciation they deserve in the signal processing literature. Whereas, based on the hypothesis of absolutely summable elements, which relies on an extension of the notion of asymptotic equivalence between matrix sequences established by Gray [16], the proof given in [18] is within the reach of most of the readers.

defined by

$$\mathbf{A}(\omega)=\begin{bmatrix} a^{1,1}(\omega) & a^{1,2}(\omega) & \cdots & a^{1,L}(\omega) \\ a^{2,1}(\omega) & a^{2,2}(\omega) & \ldots & a^{2,L}(\omega) \\ \vdots & \vdots & & \vdots \\ a^{L,1}(\omega) & a^{L,2}(\omega) & \cdots & a^{L,L}(\omega) \end{bmatrix}$$

$\mathbf{B}(\omega)$ *is defined in the same way from* $b^{u,v}(\omega)$, *with* $\min_\omega \lambda_L\{\mathbf{B}(\omega)\}=m_b>0$. *Then, for all continuous functions* F *on* $I_\omega=[m,M]$ *with* $m\overset{\text{def}}{=}\min_\omega \lambda_L(\mathbf{B}^{-1}(\omega)\mathbf{A}(\omega))$ *and* $M\overset{\text{def}}{=}\max_\omega \lambda_1(\mathbf{B}^{-1}(\omega)\mathbf{A}(\omega))$

$$\lim_{K\to\infty}\frac{1}{K}\sum_{u=1}^{KL}F(\lambda_u(\mathbf{B}_{K,L}^{-1}\mathbf{A}_{K,L})) = \frac{1}{2\pi}\int_{-\pi}^{\pi}\sum_{u=1}^{L}F(\lambda_u(\mathbf{B}^{-1}(\omega)\mathbf{A}(\omega))\,d\omega$$

From this theorem, we prove the following corollary in Appendix A:

Corollary 1. *The largest generalized eigenvalue of* $(\mathbf{A}_{K,L},\mathbf{B}_{K,L})$ *is convergent in* K *and*

$$\lim_{K\to\infty}\lambda_1(\mathbf{B}_{K,L}^{-1}\mathbf{A}_{K,L})=\max_\omega \lambda_1(\mathbf{B}^{-1}(\omega)\mathbf{A}(\omega))$$

The assumptions of Theorem 1 and Corollary 1 apply for the sequence of the space–time covariance matrices $(\bar{\mathbf{R}}_{s,K},\bar{\mathbf{R}}_{i+n,K})$ w.r.t. the number K of taps:

$$\lim_{K\to\infty}\mathrm{SINR}(K)=\max_{f\in[-B/2;B/2]}\{\lambda_1(\mathbf{R}_{i+n}^{-1}(f)\mathbf{R}_s(f))\}$$

Then, since $\mathbf{R}_{i+n}^{-1}(f)\mathbf{R}_s(f)$ has rank one, it has the following single non-zero eigenvalue

$$\mathscr{S}_s(f)\boldsymbol{\phi}(\theta_s,f)^H\mathbf{R}_{i+n}^{-1}(f)\boldsymbol{\phi}(\theta_s,f)$$

associated with the eigenvector $\mathbf{R}_{i+n}^{-1}(f)\boldsymbol{\phi}(\theta_s,f)$ and we obtain the following result:

Result 1. For optimal space–time beamforming sampled at the Shannon rate, the SINR tends to the following expression when the number K of taps increases to infinity

$$\lim_{K\to\infty}\mathrm{SINR}(K)=\max_{f\in I_f}\{\mathscr{S}_s(f)\boldsymbol{\phi}(\theta_s,f)^H\mathbf{R}_{i+n}^{-1}(f)\boldsymbol{\phi}(\theta_s,f)\} \tag{6}$$

where $\mathbf{R}_{i+n}(f)$ is defined by (3) and where $I_f=[-B/2;B/2]$.

At first glance, this SINR tends to the maximum zero-bandwidth optimal spatial SINR associated with a frequency f_m in the band I_f. And consequently, this optimal asymptotic space–time beamformer has the same behavior as an infinitely narrow bandpass filter at f_m followed by an optimal zero-bandwidth spatial beamformer.

But, we have to elaborate a little bit. Thus, let us compare this optimal asymptotic space–time SINR (6) obtained for $f=f_m\in I_f$ with the zero-bandwidth optimal spatial SINR corresponding to the demodulation frequency f_0+f_m associated with the same signal of interest, interference and noise powers σ_s^2, σ_j^2 and σ_n^2. We see from (3) that this optimal asymptotic space–time SINR (6) is associated with a zero-bandwidth optimal spatial SINR corresponding to signal, interference and noise powers $B\mathscr{S}_s(f_m)$, $B\mathscr{S}_j(f_m)$ and σ_n^2, respectively. Furthermore, the associated steering vectors $\boldsymbol{\phi}(\theta_s,f_m)$ and $\boldsymbol{\phi}(\theta_j,f_m)$ depend on the inter-element spacing of the array which generally is related to $f_0+B/2$ (Shannon sampling condition) or sometimes to f_0 for the space–time SINR, whereas this inter-element spacing would have probably been chosen as a function of f_0+f_m in the context of narrowband beamforming around frequency f_0+f_m. However, for temporally white signals of interest, some properties can be proved.

In the case of oversampling with respect to Shannon rate ($T<1/B$), the spectral matrices $\mathbf{R}_s(f)$ and $\mathbf{R}_{i+n}(f)$ are both bandlimited to $[-B/2,B/2]\subset[-1/2T,1/2T]$, and consequently $\min_f \lambda_L(\mathbf{R}_{i+n}(f))=0$ and the technical condition on which Theorem 1 is derived is no longer valid. Furthermore, in this case, Theorem 1 has no meaning because the generalized eigenvalues of $(\mathbf{R}_s(f),\mathbf{R}_{i+n}(f))$ are not defined for $B/2<|f|\leqslant 1/2T$. In these conditions, proving Result 1 is an open problem which is challenging. However, extensive numerical experiments show that Result 1 extends to that case (see Section 4.3).

3.3. Expression of the asymptotic SINR for temporally white signals of interest

Suppose now that the signal of interest and the multichannel interferer are temporally white. With $S_j(f)=\sigma_j^2/B$ and $S_{j,j'}(f)=\sigma_{j,j'}/B$, the generating function $\mathbf{R}_{i+n}(f)$ defined in (3) can be written at frequency $f=0$ as

$$\mathbf{R}_{i+n}(0)=\frac{1}{B}\left(\sum_{j=1}^{J}\sigma_j^2\boldsymbol{\phi}(\theta_j,0)\boldsymbol{\phi}(\theta_j,0)^H + \sum_{1\leqslant j\neq j'\leqslant J}\sigma_{j,j'}\boldsymbol{\phi}(\theta_j,0)\boldsymbol{\phi}(\theta_{j'},0)^H+\sigma_n^2\mathbf{I}\right)$$

which is (up to the multiplicative term $1/B$) the interference plus noise spatial covariance matrix $\mathbf{R}_{i+n}$ associated with zero-bandwidth signals around frequency f_0 with the same powers and correlations. Consequently from (6), we obtain

$$\lim_{K\to\infty}\mathrm{SINR}(K)\geqslant\sigma_s^2\boldsymbol{\phi}(\theta_s)^H\mathbf{R}_{i+n}^{-1}\boldsymbol{\phi}(\theta_s)$$

with $\boldsymbol{\phi}(\theta_s)\overset{\text{def}}{=}\boldsymbol{\phi}(\theta_s,0)$, which is the optimal SINR given for zero-bandwidth spatial beamformers around f_0 (e.g., see [4, rel.6.66]). Thus, we have proved the following result:

Result 2. For temporally white signal of interest and multichannel interferer, the asymptotic SINR at the output of the optimal space–time beamformer is larger than the SINR at the output of the optimal spatial beamformer associated with zero-bandwidth signals around frequency f_0 with same spatial correlations and powers.

Therefore, for a finite number K of taps, the optimal space–time beamformer can outperform the zero-bandwidth optimal spatial SINR. This point that has never been reported in the literature, will be illustrated in Section 4.1.

We now analyze the particular situation of interference whose spectra cancel at least at a common frequency. In this particular case, the following result is proved in Appendix B:

Result 3. In the presence of several interferers whose spectra share at least a common frequency null ν_0 and a temporally white signal of interest of power σ_s^2, we have

$$\lim_{K\to\infty} \mathrm{SINR}(K) = \frac{\sigma_s^2}{\sigma_n^2} L$$

This result means that in the presence of interference with at least one common zero in their spectra, space–time processing allows one to reach asymptotically the SINR corresponding to an interference-free context. Let us note that though the asymptotic notion is purely theoretical, we will see in Section 4.2 that in most practical cases, a small value of the number of taps is sufficient to reach near optimal performance.

4. Illustrative examples

This section illustrates Result 2 through numerical experiments and complements the last two results by exhibiting the speed of convergence of the optimal SINR for a limited number of taps to its asymptotic value for both white and bandlimited interference. Moreover, in the latter case, the influence of the fractional bandwidth is examined. Finally, we examine the influence of the time sampling rate on the optimal space–time SINR. We consider throughout this section a uniform linear array with only one interference source where

$$\boldsymbol{\phi}(\theta,f) = [1, e^{j\pi((f_0+f)/f_0)u}, \ldots, e^{j(L-1)\pi((f_0+f)/f_0)u}]^T$$

with $u = \sin(\theta)$ ($u_s = \sin(\theta_s)$ and $u_j = \sin(\theta_j)$ for the signal of interest and the interference, respectively). The signal of interest is white in the band $[-B/2; B/2]$. In all the simulations, $u_j = 0.3$, $\sigma_n^2 = 0\,\mathrm{dB}$ and $\sigma_s^2 = 0\,\mathrm{dB}$.

4.1. White interference case

In this section, we suppose that the interference is white in the band $[-B/2; B/2]$. Thus

$$\lim_{K\to\infty} \mathrm{SINR}(K) = \max_{f\in I_f} \left\{ \frac{\sigma_s^2}{\sigma_n^2} L \left(1 - \frac{\sigma_j^2 |\boldsymbol{\phi}(\theta_1,f)^H \boldsymbol{\phi}(\theta_s,f)|^2}{L(\sigma_n^2 + L\sigma_j^2)} \right) \right\} \tag{7}$$

Fig. 1exhibits the asymptotic optimal space–time SINR for different values of the fractional bandwidth B/f_0 and the optimal spatial zero-bandwidth SINR in the conditions of Result 2, with $L = 4$ and $\sigma_j^2 = 10$. We check that the increase of the fractional bandwidth leads to a reduction of the SINR loss width around the interferer. More precisely, it is straightforward from (7) to prove that the asymptotic optimal space–time SINR presents a notch behavior around the signal of interest's DOA, whose width $4/L(1 + B/2f_0)$ shrinks when the fractional bandwidth increases. Furthermore from (7), the sidelobe's effects disappear for $1 + B/2f_0 > 2(1 - B/2f_0)$, i.e., for $B/f_0 > 2/3$.

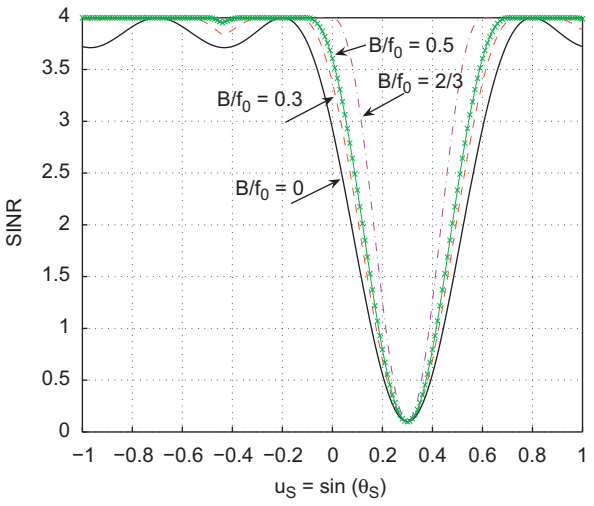

Fig. 1. Optimal asymptotic space–time SINR for different values of the fractional bandwidth, and optimal spatial zero-bandwidth SINR ($B/f_0 = 0$) as a function of the signal of interest's DOA.

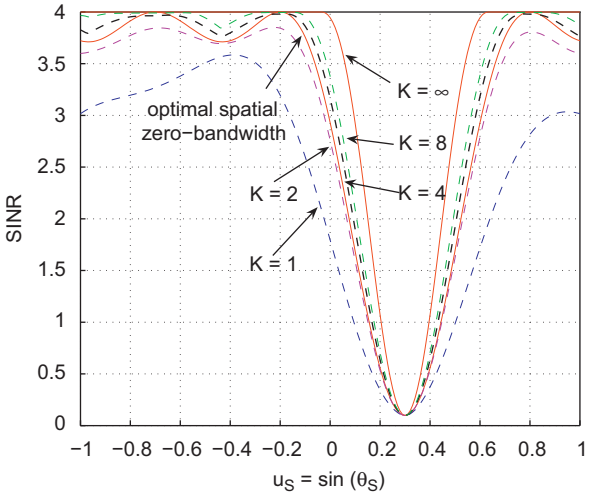

Fig. 2. Optimal space–time SINR for different values of the number of taps and optimal spatial zero-bandwidth SINR, as a function of the signal of interest's DOA.

Moreover, we see from Fig. 1 that the asymptotic optimal space–time SINR outperforms the optimal spatial zero-bandwidth SINR for all fractional bandwidths and signal of interest's DOA, except at the DOA of the interferer. Naturally the impact of these properties reduces for scenarios for which $L(L + \sigma_n^2/\sigma_j^2) \gg 1$ (7), where the two SINR are very close, as it will be illustrated in Fig. 3. Fig. 2 compares the optimal space–time SINR to the optimal spatial SINR for $B/f_0 = 0.5$ at different numbers K of taps. It shows that the optimal space–time SINR begins outperforming the optimal spatial SINR from only four taps.

From now on, $L = 16$ and $\sigma_j^2 = 30\,\mathrm{dB}$. In Fig. 3, we plot the optimal space–time SINR for different values of the number K of taps, with $B/f_0 = 0.3$. First we check that the SINR converges to the asymptotic SINR given by Result 1,

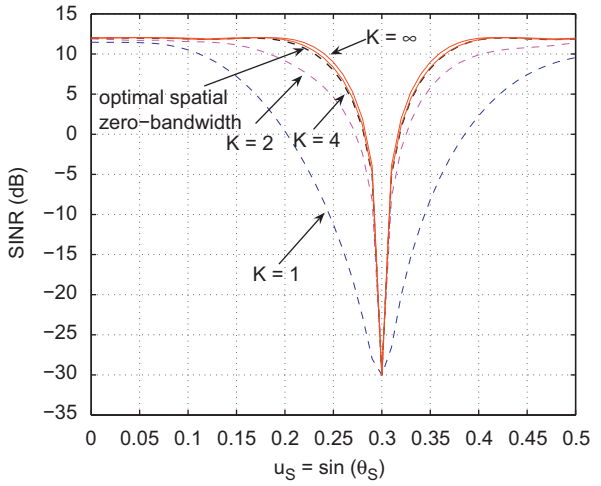

Fig. 3. Optimal space–time SINR for different values of the number of taps and optimal spatial zero-bandwidth SINR, as a function of the signal of interest's DOA.

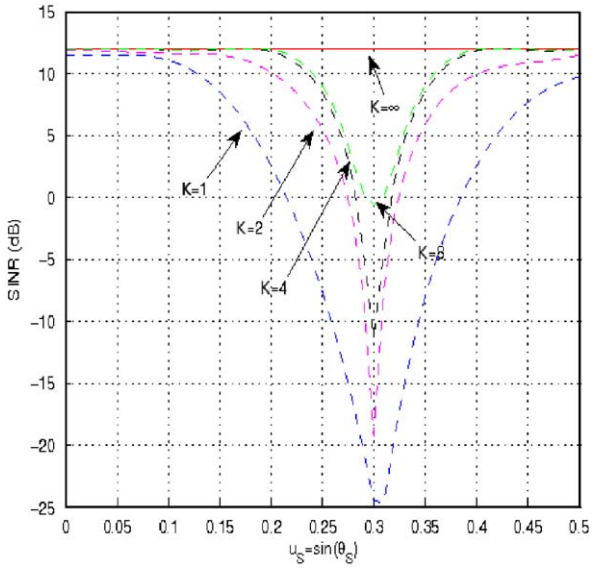

Fig. 4. Optimal space–time SINR for different values of the number of taps, as a function of the signal of interest's DOA for $b = 3B/4$.

which is close to the associated optimal spatial SINR. Then, we notice that the convergence is rapid, since the asymptotic bound is nearly reached with $K = 4$.

4.2. Bandlimited white interference case

Let us suppose that the interference has constant PSD in the band $[-b/2; b/2]$ with $b < B$. We illustrate the speed of convergence of the optimal space–time SINR for a given number of taps to the asymptotic upper-bound given by Result 2. Thus, we plot in Figs. 4 and 5 the optimal space–time SINRs for $b = \frac{3}{4}B$ and $b = B/2$, respectively (dashed plots), at given number of taps and compare them

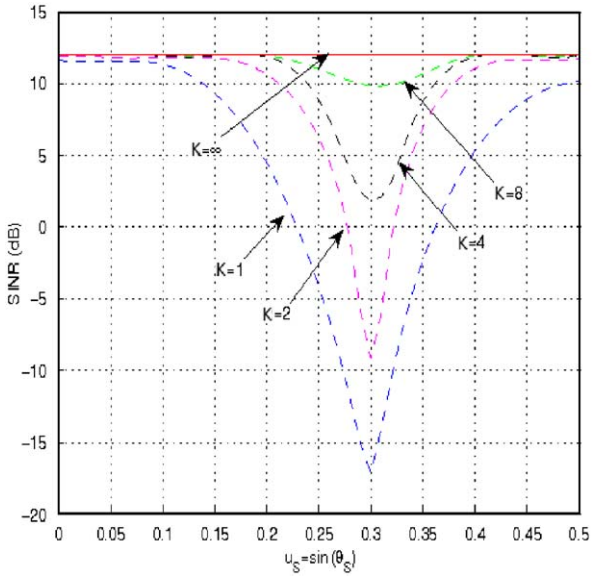

Fig. 5. Optimal space–time SINR for different values of the number of taps, as a function of the signal of interest's DOA for $b = B/2$.

to the asymptotic optimal space–time SINR (solid plot). Let us note that the case $K = 1$ corresponds to spatial processing and that the SINR degrades when b increases. In both figures, we check that the optimal SINR (asymptotically w.r.t. the number of taps) is equal to $\sigma_s^2/\sigma_n^2 L$ and that the optimal space–time SINRs converge with the number of taps to the asymptotic optimal space–time SINR. Then, we note that the convergence speed increases when the interference bandwidth decreases. For instance, we observe in Fig. 5 (where $b = B/2$) that the optimal space–time SINR with $K = 4$ taps outperforms the optimal space–time SINR with $K = 8$ taps of Fig. 4 (where $b = 3B/4$).

4.3. Influence of the time sampling frequency

Now, we examine the influence of the time sampling rate on the optimal space–time SINR. In Fig. 6, we plot the optimal space–time SINR for two values of the temporal sampling period, i.e., $T = 1/B$ and $T = 1/2B$ and different values of the number of taps for a white interference in the band $[-B/2, B/2]$.

First, we observe that in both cases, the SINR seems to converge to the asymptotic SINR given by Result 1, although this result has been proved only for $T = 1/B$. However, we note that the convergence is much faster for $T = 1/2B$ than for $T = 1/B$. Consequently, oversampling w.r.t. the Shannon sampling rate allows one to improve the performance for a given number of taps. We note that extensive experiment confirms these observations. Let us note that the influence of the time sampling rate has been analyzed in [10] for a bandpass tapped delay line implementation of the MMSE algorithm in the case of a two-sensor array. In this paper, the author has also noticed the improvement of performance in terms of SINR due to the use of oversampling, for an array in which each

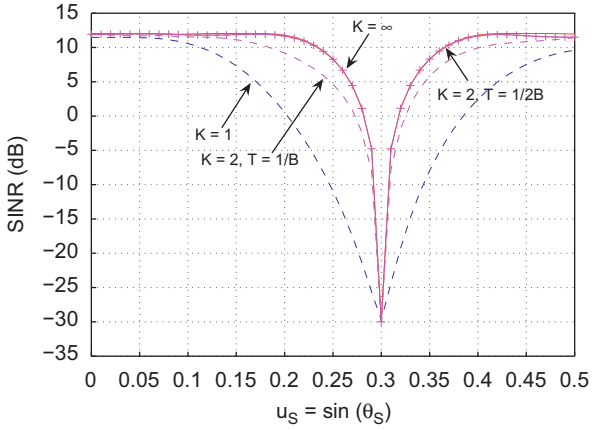

Fig. 6. Optimal space–time SINR with $T = 1/B$ (- -) and $T = 1/2B$ (-+-) for different values of the number of taps, as a function of the target's DOA.

element has only two weights. The physical interpretation is that oversampling increases the correlation between interference components which makes their nulling easier.

Appendix A. Proof of Corollary 1

We mimic here the approach of [16, Corollary 4.2] that we recall for the convenience of the reader. First, note that for all K, the KL eigenvalues of $\mathbf{B}_{K,L}^{-1}\mathbf{A}_{K,L}$ lie in I_ω and the L eigenvalues of $\mathbf{B}^{-1}(\omega)\mathbf{A}(\omega)$ are continuous in $[-\pi,\pi]$.

Define the complementary distribution eigenvalue function $D_K(x) \stackrel{\text{def}}{=} (\text{number of } \lambda_u(\mathbf{B}_{K,L}^{-1}\mathbf{A}_{K,L}) \geqslant x)/K$ which is given by $(1/K)\sum_{u=1}^{KL} \mathbb{1}_{[x,M]}(\lambda_u(\mathbf{B}_{K,L}^{-1}\mathbf{A}_{K,L}))$, where

$$\mathbb{1}_{[x,M]}(\alpha) \stackrel{\text{def}}{=} \begin{cases} 1 & \text{for } \alpha \in [x,M] \\ 0 & \text{elsewhere} \end{cases} \quad \text{with } x < M$$

Using two continuous functions on I_ω that provide upper and lower bounds to the indicator function $\mathbb{1}_{[x,M]}(\alpha)$ and converge to it in the limit, and applying Theorem 1 to these two continuous functions, we straightforwardly obtain

$$\lim_{K\to\infty} D_K(x) = \frac{1}{2\pi}\sum_{u=1}^{L} \int_{\omega\in[-\pi,\pi], x\leqslant\lambda_u(\mathbf{B}^{-1}(\omega)\mathbf{A}(\omega))\leqslant M} d\omega$$

Consequently, $\lim_{K\to\infty} D_K(M-\varepsilon) = (1/2\pi)\sum_{u=1}^{L} \int_{\omega\in[-\pi,\pi],\ M-\varepsilon\leqslant\lambda_u(\mathbf{B}^{-1}(\omega)\mathbf{A}(\omega))\leqslant M} d\omega > 0$ where the strict inequality follows from the continuity of the L eigenvalues of $\mathbf{B}^{-1}(\omega)\mathbf{A}(\omega)$ in $[-\pi,\pi]$. Since $\lim_{K\to\infty}(\text{number of } \lambda_u(\mathbf{B}_{K,L}^{-1}\mathbf{A}_{K,L}) \in [M-\varepsilon, M])/K > 0$, there must be eigenvalues of $\mathbf{B}_{K,L}^{-1}\mathbf{A}_{K,L}$ in the interval $[M-\varepsilon, M]$ for arbitrary small ε. Noting that the space–time setting with K taps is a special case of a processor with $K+1$ taps where the $K+1$th tap weight is set to zero in each channel, we obtain by the inclusion principle in (5) that the larger generalized eigenvalues of $(\mathbf{A}_{K,L}, \mathbf{B}_{K,L})$, $\lambda_1(\mathbf{B}_{K,L}^{-1}\mathbf{A}_{K,L})$ increases with K (L fixed). Consequently, this proves Corollary 1.

Appendix B. Proof of Result 2

First, note that if $\mathscr{S}_j(v_0) = 0$ for $j = 1,\ldots,J$ with $v_0 \in [-B/2, B/2]$, using $|\mathscr{S}_{j,j'}(f)|^2 \leqslant \mathscr{S}_j(f)\mathscr{S}_{j'}(f)$, the different cross power spectral densities $(\mathscr{S}_{j,j'}(f))_{j\neq j'=1..J}$ cancel at v_0 as well. Consequently $\mathbf{R}_{i+n}(v_0) = (\sigma_n^2/B)\mathbf{I}$ from (3). Then from (6), we obtain

$$\lim_{K\to\infty} \text{SINR}(K) \geqslant \frac{\sigma_s^2}{B}\boldsymbol{\phi}(\theta_s, v_0)^H \mathbf{R}_{i+n}^{-1}(v_0)\boldsymbol{\phi}(\theta_s, v_0) = \frac{\sigma_s^2}{\sigma_n^2}\|\boldsymbol{\phi}(\theta_s, v_0)\|^2 = \frac{\sigma_s^2}{\sigma_n^2}L$$

Now, we prove that the limit of SINR(K) is upper bounded by $(\sigma_s^2/\sigma_n^2)L$. Using $\tilde{\mathbf{R}}_{i+n,K} \geqslant \sigma_n^2\mathbf{I}$, we have

$$\text{SINR}(K) \leqslant \frac{\mathbf{w}_K^H \tilde{\mathbf{R}}_{s,K}\mathbf{w}_K}{\sigma_n^2\|\mathbf{w}_K\|^2} \leqslant \frac{\lambda_1(\tilde{\mathbf{R}}_{s,K})}{\sigma_n^2} \tag{8}$$

where $\tilde{\mathbf{R}}_{s,K}$ is block-Toeplitz structured. Applying [19, Theorem 3], dedicated to the limit of the largest eigenvalue of block-Toeplitz matrices with non-Toeplitz blocks where the number K of block tends to infinity, we have[3]

$$\lim_{K\to\infty} \lambda_1(\tilde{\mathbf{R}}_{s,K}) = B\lambda_1(\mathbf{R}_s(f))$$

where the largest eigenvalue of the rank one matrix $\mathbf{R}_s(f)$ (4) is $(\sigma_s^2/B)L$. Consequently

$$\lim_{K\to\infty} \text{SINR}(K) \leqslant \frac{\sigma_s^2}{\sigma_n^2}L$$

which proves Result 3.

References

[1] M. Zatman, How narrow is narrowband?, IEE Proc. Radar Sonar Navig. 145 (April 1998) 85–91.
[2] J. Hudson, Adaptive Array Principles, Peter Peregrinus, London, 1981.
[3] M. Oudin, J.P. Delmas, Robustness of adaptive narrowband beamforming with respect to bandwidth, IEEE Trans. Signal Process. 56 (April 2008) 1532–1538.
[4] H.L. Van Trees, Optimum Array Processing, Part IV of Detection, Estimation and Modulation Theory, Wiley Interscience, New York, 2002.
[5] W.E. Rodgers, R.T. Compton, Adaptive array bandwidth with tapped delay-line processing, IEEE Trans. Aerospace Electron. Syst. January 15 (1979) 21–27.
[6] J.T. Mayhan, A.J. Simmon, W.C. Cummings, Wideband adaptive antenna nulling using tapped delay-lines, IEEE Trans. Antennas Propagat. 29 (November 1981) 923–936.
[7] L.C. Godara, M.R.S. Jahromi, Limitations and capabilities of frequency domain broadband constrained beamforming schemes, IEEE Trans. Signal Process. 47 (September 1999) 2386–2395.
[8] Y.S. Kim, I.M. Weiss, Bandwidth performance of a 16-element thinned phased array with tapped delay-line filter, IEEE Trans. Antennas Propagat. 39 (April 1991) 562–565.
[9] F.W. Vook, R.T. Compton, Bandwidth performance of linear arrays with tapped delay-line processing, IEEE Trans. Aerospace Electron. Syst. 28 (July 1992) 901–908.
[10] R.T. Compton, The bandwidth performance of a two-element adaptive array with tapped delay-line processing, IEEE Trans. Antennas Propagat. 36 (January 1988) 5–14.
[11] M.S. Brandstein, D.B. Ward (Eds.), Microphone Arrays: Signal Processing Techniques and Applications, Springer, Berlin, 2001.

[3] The period B is introduced to be consistent with [19, Theorem 3], where the period in ω is 2π.

[12] L.C. Godara, Application of the fast Fourier transform to broadband beamforming, J. Acoust. Soc. Am. 98 (July 1995) 230–239.
[13] L.C. Godara, M.R.S. Jahromi, Performance of broadband arrays using convolution constraints, in: Proceedings of the Eighth International Symposium on Signal Processing and its Applications, vol. 1, August 2005, pp. 419–422.
[14] H. Duan, B.P. Ng, L.M. See, Broadband beamforming using TDL-IIR filters, IEEE Trans. Signal Process. 55 (March 2007) 990–1002.
[15] U. Grenander, G. Szegö, Toeplitz Forms and Their Applications, Chelsea, New York, 1984.
[16] R.M. Gray, Toeplitz and circulant matrices: a review, Found. Trends Commun. Inf. Theory 2 (2006) 155–239.
[17] S. Serra, Spectral and computational analysis of block Toeplitz matrices having non-negative definite matrix-valued generating functions, BIT 39 (1) (1999) 152–175.
[18] M. Oudin, J.P. Delmas, Asymptotic generalized eigenvalue distribution of block multilevel Toeplitz matrices, IEEE Trans. Signal Process. 57 (1) (2009) 382–387.
[19] H. Gazzah, P.A. Regalia, J.P. Delmas, Asymptotic eigenvalue distribution of block Toeplitz matrices and application to blind SIMO channels identification, IEEE Trans. Inf. Theory 47 (3) (March 2001) 1243–1251.